

Odd-Even Effects in Pre-Equilibrium Processes*

S. M. Grimes, J. D. Anderson, J. W. McClure, B. A. Pohl, and C. Wong

Lawrence Livermore Laboratory, Livermore, California 94550

(Received 18 August 1972)

Neutron spectra produced by the (p, n) reaction at 12 and 14 MeV on targets of ^{112}Cd , ^{113}Cd , ^{114}Cd , and ^{115}In are compared with the predictions of the exciton model for pre-equilibrium reactions. It is concluded that although the shape of the spectra for even- A targets differs from that for odd- A targets, the differences are not entirely consistent with the analysis of Lee and Griffin for (p, n) reactions on the Sn isotopes. The possible explanations for deviations from model calculations include effects due to shells, pairing, and angular momentum.

I. INTRODUCTION

Although the exciton model¹ for pre-equilibrium processes has been studied²⁻¹⁷ both experimentally and theoretically, relatively little attention has been paid to the prediction¹ that systematic differences between the shapes of spectra produced in (p, n) reactions on even- A and odd- A targets should occur. Verbinski and Burrus³ assumed that such differences exist and used the formulas proposed by Griffin¹ to analyze their data, which included spectra from both even- and odd- A targets. They did not test the prediction by obtaining spectra for targets adjacent in A , however, and the focus of their investigation was more on separating the contributions of various reaction mechanisms than on comparisons of the pre-equilibrium spectra shapes for various targets. The other papers have also concentrated on establishing the basic characteristics of the pre-equilibrium mechanism and have not attempted to compare spectra from even- and odd- A targets in detail.

Recently Lee and Griffin¹⁸ analyzed data¹⁹ from the $^{118}\text{Sn}(p, n)$ and $^{117}\text{Sn}(p, n)$ reactions and concluded that the predicted odd-even differences are observed. The present measurements were undertaken to see if spectra for other targets in this mass region show similar characteristics. The reactions studied included $^{112}\text{Cd}(p, n)$, $^{113}\text{Cd}(p, n)$, $^{114}\text{Cd}(p, n)$, and $^{115}\text{In}(p, n)$. This group is adjacent to the pair of targets analyzed by Lee and Griffin and includes two even- A and two odd- A targets.

II. EXPERIMENTAL PROCEDURE

Solid self-supporting targets of Cd and In were bombarded with the proton beam of the Livermore 2.3-m cyclotron. A description of the experimental equipment and procedures has been published previously.²⁰ Spectra at nine angles be-

tween 15 and 135° were obtained simultaneously with the use of a multidetector array; time-of-flight spectroscopy with a 10.8-m flight path yielded the energy distribution of the neutrons. Typical energy spectra are presented in Figs. 1 and 2.

III. ANALYSIS AND RESULTS

The basic assumption of the exciton model is that the equilibration process of the compound nucleus proceeds by a series of two-body interactions. If the level densities for various particle-hole states are calculated from a basis of equidistant single-particle levels and if transitions to more complicated configurations (involving one additional particle-hole state) are much more probable than are transitions to states with the same or a smaller number of particles and holes,

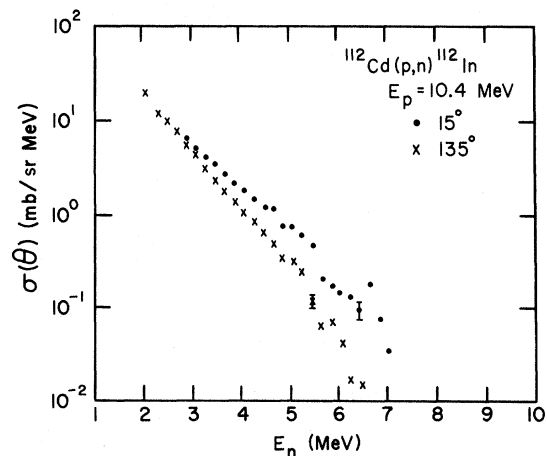


FIG. 1. The differential cross section for the $^{112}\text{Cd}(p, n)^{112}\text{In}$ reaction at a bombarding energy of 10.4 MeV as a function of center-of-mass neutron energy. The symbols \bullet and \times denote data points at 15° and 135°, respectively. Indicated errors are statistical only.

the following result is obtained⁵:

$$\sigma(\epsilon) \propto \frac{\epsilon \sigma_{\text{inv}}}{(gE^*)^3} \sum_{\substack{n=n_0 \\ \Delta n=2}} \left(\frac{U}{E^*}\right)^{n-2} (n^3 - n). \quad (1)$$

In this expression $\sigma(\epsilon)$ is the cross section for emission of a particle with energy ϵ , σ_{inv} is the inverse capture cross section, g is the density of single-particle states, E^* is the excitation energy in the compound system, and U is the energy in the residual nucleus. The parameter n corresponds to the exciton number (where an exciton denotes either a particle or a hole) of the state from which decay occurs. The power series results from the assumption that each of the pre-equilibrium states formed during the approach to equilibrium has a decay width for particle emission. For values of the residual excitation energy such that U/E^* is small, the first term of Eq. (1) would be expected to dominate. In this case, Eq. (1) may be rewritten

$$\sigma(\epsilon) \propto \epsilon \sigma_{\text{inv}} \rho_{n-1}(U), \quad (2)$$

where $\rho_{n-1}(U)$ is the density of excited levels of $n-1$ exciton character at an excitation energy U . This form shows the analogy with the corresponding form for equilibrium decay of the compound nucleus:

$$\sigma(\epsilon) \propto \epsilon \sigma_{\text{inv}} \rho(U), \quad (3)$$

where $\rho(U)$ is the level density of the residual nucleus.

More generally, it is expected that both equilibrium and pre-equilibrium processes could contribute to a given spectrum, in which case

$$\sigma(\epsilon) \propto \epsilon \sigma_{\text{inv}} (\alpha \rho(U) + \beta \rho_{n-1}(U)). \quad (4)$$

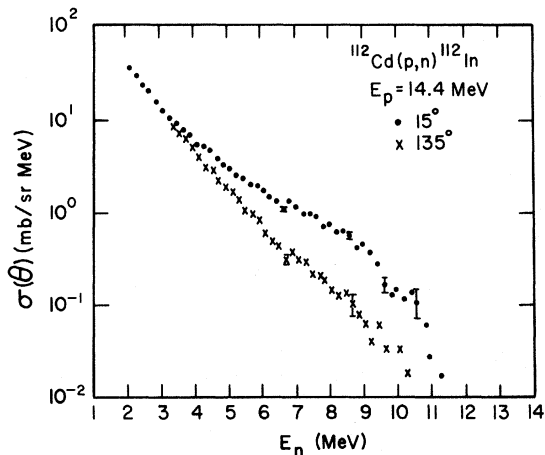


FIG. 2. Same as Fig. 1, except that the bombarding energy is 14.4 MeV.

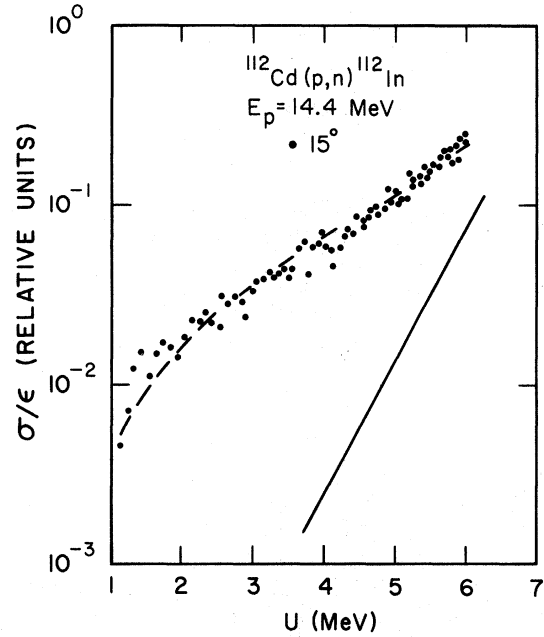


FIG. 3. Best fit (dashed line) of the form $A\rho(U) + BU^n$ to the 15° $^{112}\text{Cd}(p,n)^{112}\text{In}$ spectrum at $E_p = 14.4$ MeV. The best fit corresponded to an n value of 2. Indicated by the solid line is the estimated contribution (equilibrium processes) from the first term of Eq. (4).

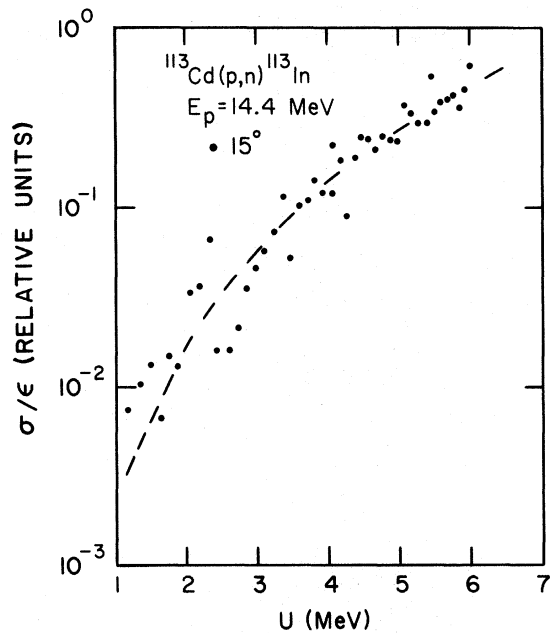


FIG. 4. Best fit (dashed line) of the form $A\rho(U) + BU^n$ to the 15° $^{113}\text{Cd}(p,n)^{113}\text{In}$ spectrum at 14.4 MeV. An n value of three produced the best fit.

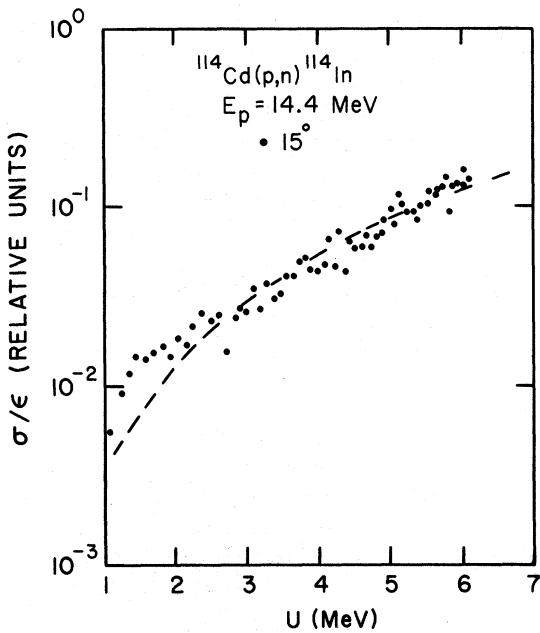


FIG. 5. Same as Fig. 4 for the $^{114}\text{Cd}(p, n)^{114}\text{In}$ reaction. In this case the best-fit value of n was 2.

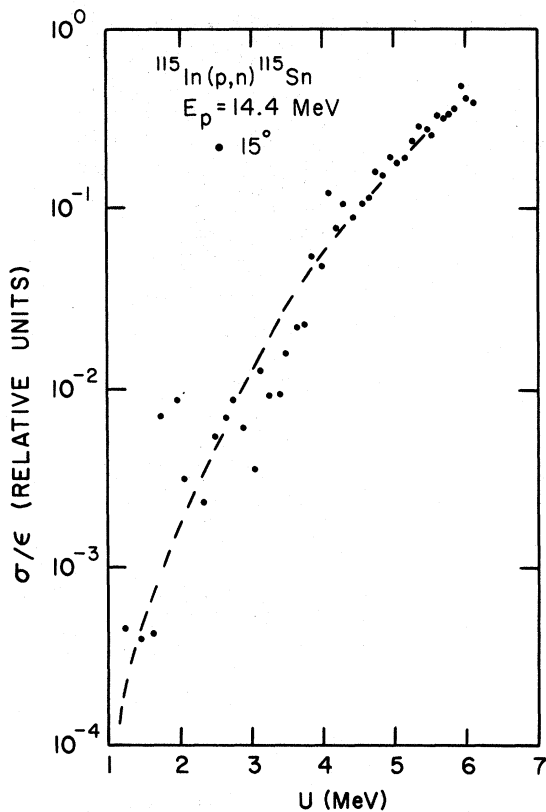


FIG. 6. Same as Fig. 4 for the $^{115}\text{In}(p, n)^{115}\text{Sn}$ reaction. The best-fit value of n was 5.

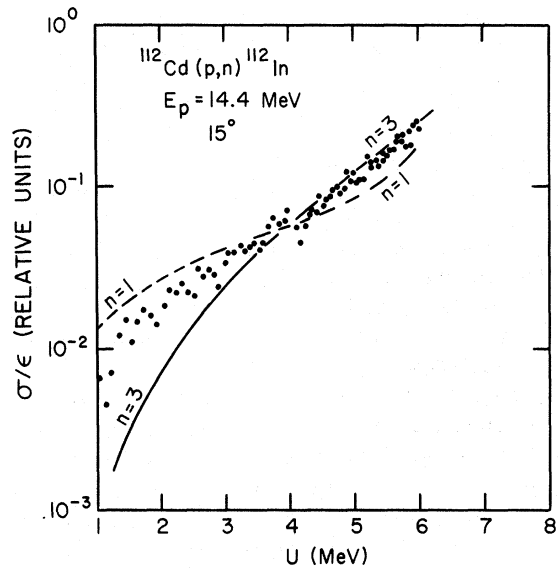


FIG. 7. Fits of the form $A\rho(U) + BU^n$ to the 15° $^{112}\text{Cd}(p, n)^{112}\text{In}$ spectrum for $n=1$ (dashed line) and $n=3$ (dot-dashed line). The best-fit value for n was 2, as shown in Fig. 3; the two fits presented here show the variation in quality of fit as a function of n .

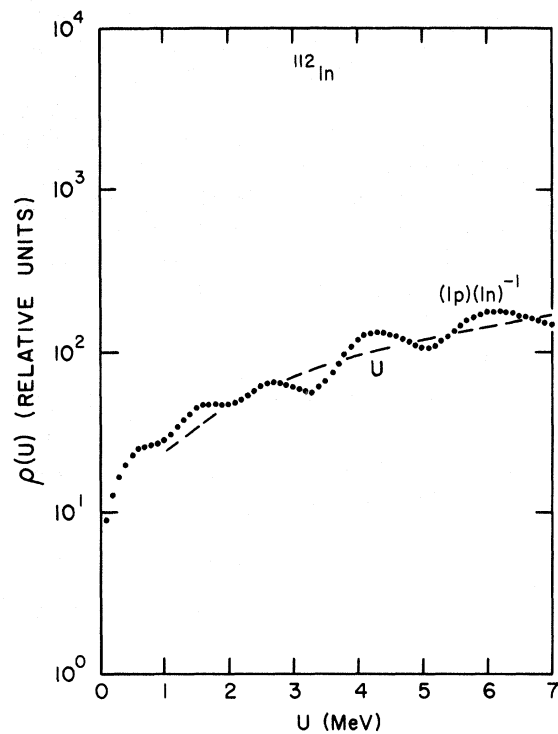


FIG. 8. The calculated one-proton-particle-one-neutron-hole state density for ^{112}In . The dashed line represents the best fit ($n=1$) of the form U^n to the calculated values.

Because α and β have different bombarding energy dependences, the shape of the spectrum as a function of U should change with bombarding energy, if both α and β are nonzero. For low bombarding energies, it is expected that equilibrium reactions will dominate the spectrum; in this region the shape observed should correspond to the first term of Eq. (4). Spectra were obtained at proton energies of 8, 9, and 10 MeV to test this prediction and a consistent shape was obtained at 8, 9, and at the backward angles for 10 MeV. As the energy is increased, contributions from the second term will become observable and eventually dominate those from the first term. The data were analyzed with the techniques described in Ref. 6. Spectra from the lowest-energy bombardments were fitted with Fermi-gas and constant-temperature parameters. These parameters were then used for the form of $\rho(U)$ in the fits of Eq. (4) to the higher-energy data ($E_p \geq 10$ MeV). The quality of fit obtained with Eq. (4) was investigated for $\rho_{n-1}(U)$ given by U^n for $0 \leq n \leq 6$. At 10 MeV the n value corresponding to the best fit could not be determined at all angles, because of the dominance of the first term in Eq. (4). Best-fit n values for the remaining angles at 10 MeV and all angles at 12 and 14 MeV are listed in Table I. Typical fits are shown in Figs. 3–6, and Fig. 7 shows the variation in fit for a change of one unit in n in either direction from the best-fit value.

Lee and Griffin¹⁸ have suggested that the values 1 or 2 for n should be obtained for even- or odd- A targets, respectively. They point out, as was also discussed in Ref. 6, that the presence of an unpaired nucleon will not influence the shape of the spectrum unless it is rescattered in the reaction, i.e., shares the excitation energy. The

present data also show that n varies between even- and odd- A targets, but the values of n differ from those obtained by Lee and Griffin. The large value of n observed for the $^{115}\text{In}(p, n)^{115}\text{Sn}$ reaction is comparable to the value observed for the $^{98}\text{Nb}(p, n)^{98}\text{Mo}$ reaction,¹⁸ which was tentatively attributed to shell closure effects. Since the effect of shells is to introduce gaps between ground or low-lying states and higher excited states, the result is to reduce the level density for low values of U relative to that for higher values; this would then produce a shape characterized by a larger power of U than would be obtained in the absence of shell effects. The analysis of Cline and Blann⁷ led to this same conclusion.

Because both the reactions studied by Lee and Griffin¹⁸ and those examined in the present experiment lead to residual nuclei at or near closed shells, it was decided to investigate the influence of shell effects in more detail. The assumption that the single particle states were equally spaced was relaxed and single-particle states obtained from a Nilsson calculation²¹ were used as basis states. These were then combined²² to form the proton-particle neutron-hole states expected to result from a pre-equilibrium (p, n) reaction. For comparison, level densities with other exciton configurations were also calculated. The results of some of these calculations are shown in Figs. 8–10. Since it was found that the calculated level densities for ^{112}In , ^{113}In , and ^{114}In had similar energy dependences, only those for ^{112}In are shown.

The most surprising result of the calculations is that the residual nucleus ^{115}Sn is the only one which shows significant shell effects. The In isotopes show much smaller deviations from the constant-spacing model. This is attributed to the extreme sensitivity of the Nilsson calculations at

TABLE I. Best-fit n values. A half integral value for n implies that the fits for the two adjacent integers were equally good.

Reaction	E_p (MeV)	15°	30°	45°	60°	75°	90°	105°	120°	135°
$^{112}\text{Cd}(p, n)^{112}\text{In}$	10.4	2	2	2	2	1.5	2
	12.4	2	2	2	2	2.5	2	2.5	3	3
	14.4	2	2	2	2	2	2.5	3	3	3
$^{113}\text{Cd}(p, n)^{113}\text{In}$	10.4	3	3.5	3	3	3.5	4	4
	12.4	3	3	3	3.5	3.5	4	4	4	4
	14.4	3	3	3	3	3	3.5	3.5	4	4
$^{114}\text{Cd}(p, n)^{114}\text{In}$	10.4	2	2	2	2	2.5	2.5	3
	12.4	2	2	2	2.5	2	2.5	3	3	3
	14.4	2	2	2	2	2	2	2.5	3	3
$^{115}\text{In}(p, n)^{115}\text{Sn}$	10.4	4.5	5	5	5	5
	12.4	5	5	5	5	5	5	5.5	5.5	5
	14.4	5	5	5	5	5	5.5	6	5.5	6

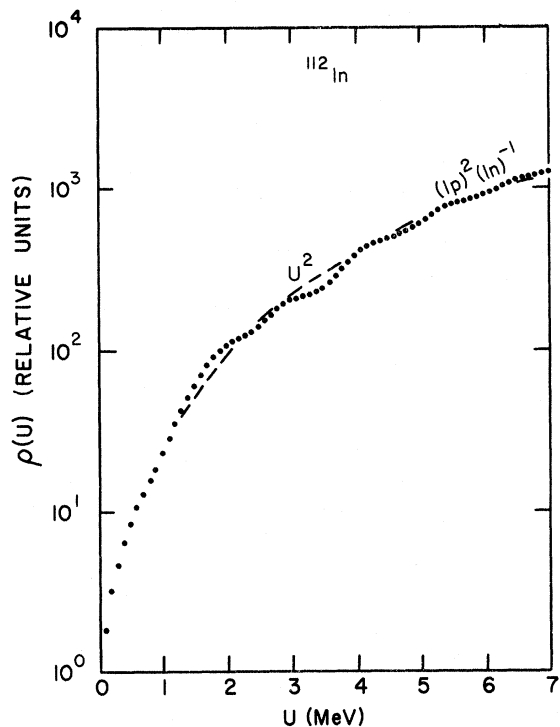


FIG. 9. Same as Fig. 8, except that the calculated density is that for two-proton-particle-one-neutron-hole states. In this case the best fit is provided by the form U^2 (dashed line).

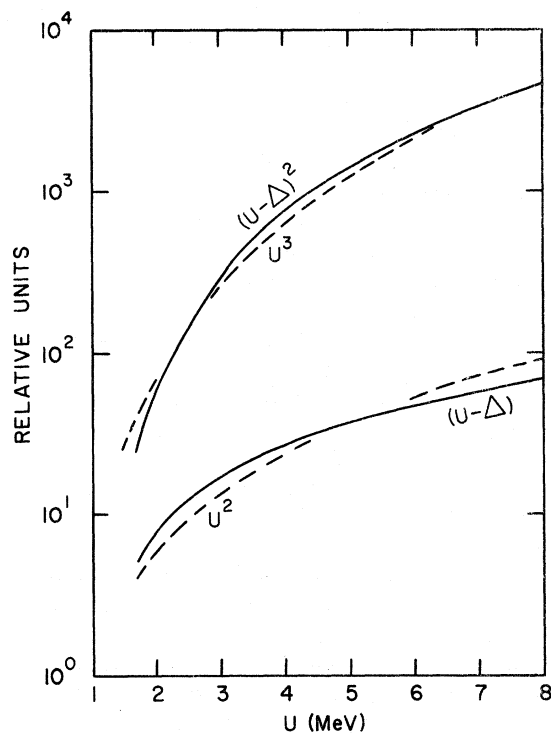


FIG. 11. Best fits of the expression U^n to the forms $U - \Delta$ and $(U - \Delta)^2$, where $\Delta = 1.2$ MeV. In each case the shifted form is fitted by a power one larger in U .

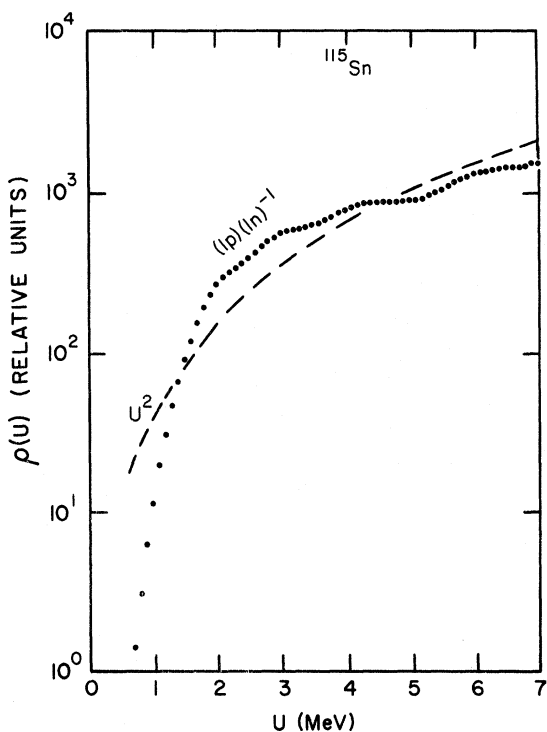


FIG. 10. Same as Fig. 8 for the residual nucleus ^{115}Sn . The best fit is obtained with the form U^2 .

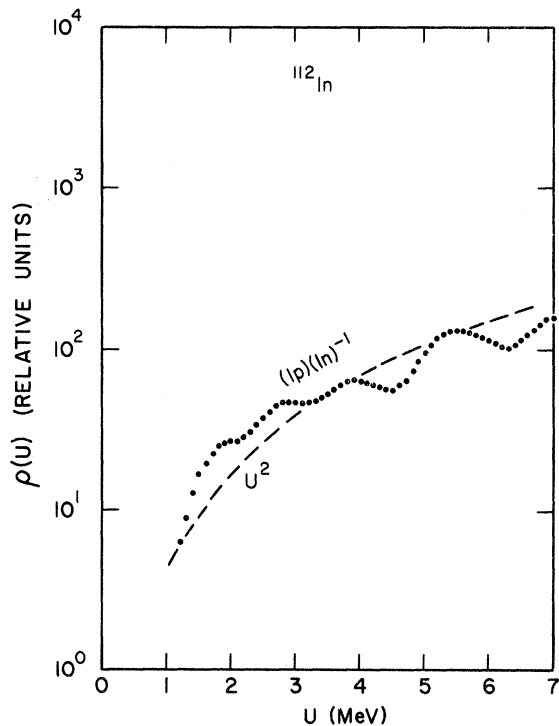


FIG. 12. Calculated one-proton-particle-one-neutron-hole density for ^{112}In shifted by 1.2 MeV. In contrast to the unshifted form (Fig. 8) the best fit of the form U^n (dashed line) is obtained for $n = 2$.

$Z = 50$ to the deformation parameter β . As can be seen from the single-particle-state diagrams,^{21, 23} the shell gap at $Z = 50$ decreases quite rapidly with increasing deformation and is gone completely for values of β of about 0.2. According to Stelson and Grodzins,²⁴ the deformation parameter increases to about this value for the Cd and Te isotopes. Thus, the deformation parameters for In, which were obtained by interpolation between Cd and Sn, are large enough to significantly reduce shell effects relative to Sn.

Clearly, some uncertainty regarding the magnitude of shell effects in the In isotopes remains, because of the difficulty of determining β and the sensitivity of the calculation to this parameter. Comparison of Figs. 8 and 10 indicates that to first-order shell effects are manifested in an energy shift; this would indicate that, to the extent shell effects have not been correctly accounted for in the calculation, additional "energy shifts" might be required to reproduce the experimental spectrum.

Inspection of the calculated densities for two-particle-one-hole states reveals that these densities are also characterized reasonably well by the functional form obtained from the constant-spacing model. This result suggests that a possible explanation for the observed U^2 or U^3 shape

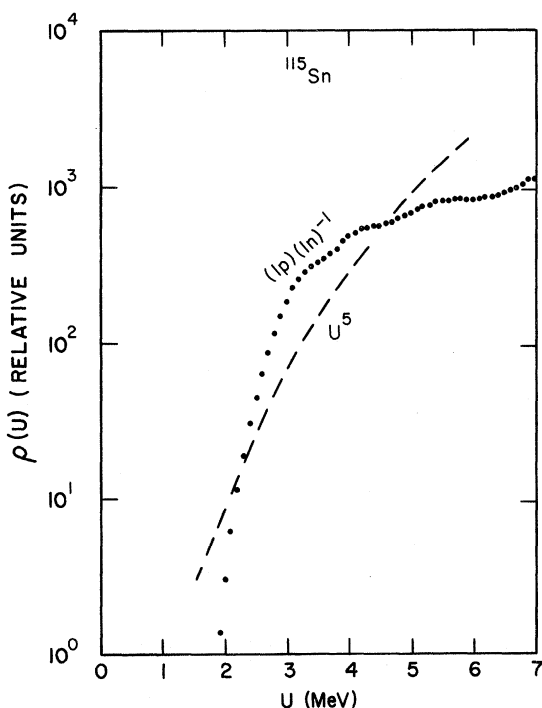


FIG. 13. Same as Fig. 12 for the residual nucleus ^{115}Sn . In this case the unshifted best-fit (Fig. 10) value is $n = 2$, while that for the shifted calculation is $n = 5$ (dashed line).

of the spectra is that the final states are not one-particle-one-hole states, but instead are more complicated states. Because a U^2 dependence is also observed for the even- A targets in the present experiments, this explanation is not consistent with the conclusions of Lee and Griffin¹⁸ that an extra scattered particle is present only for odd- A targets.

The (p, n) reaction on even- A targets leads to an odd-odd residual nucleus, while the corresponding final nucleus for an odd- A target will be either odd-even (e.g. ^{113}In) or even-odd (e.g. ^{115}Sn). Therefore, an energy shift would be expected between the spectra produced by (p, n) reactions on even- A and odd- A targets because of the need to break an additional pair in an odd- A nucleus to reach a proton-particle-neutron-hole state. Such shifts will produce spectral shapes characterized by higher values of n , just as the shell-induced shifts discussed previously. Gilbert and Cameron²⁵ propose values of the pairing energy of about 1.2 MeV in this mass range. Figs. 11–13 show the effect of a shift of this magnitude on the shape of the spectra. This shift is sufficient to raise the best-fit value of n by one unit for both the forms U and U^2 as is seen in Fig. 11. Similarly, the effect of a 1.2-MeV shift on the calculated $1p(1n)^{-1}$ densities for ^{112}In and ^{115}Sn is shown in Figs. 12 and 13. The unshifted calculations (Figs. 8 and 9) are parametrized by U and U^2 , respectively, while the best fits to the shifted values are U^2 and U^5 , which are in closer agreement with the parametrization of the data. Because both shell and pairing effects are manifested to first order in energy shifts, separation of the two is difficult but could be accomplished by studying (p, n) spectra on adjacent targets more removed from closed shells.

The role of angular momentum in pre-equilibrium reactions has not been examined but might be important for (p, n) reactions to low-lying states in this mass region. Proton particles and holes are expected to be primarily $g_{3/2}$ and $g_{7/2}$, respectively, at very low excitation energies, with contributions from $d_{5/2}$ particles and $p_{1/2}$ holes expected at somewhat higher energies. Correspondingly, neutron-hole states will be predominantly from $g_{7/2}$ at low excitation energies. Thus, the low-lying proton-particle-neutron-hole states may be characterized by somewhat higher angular momentum values than corresponding states at higher excitations, resulting in an inhibition of transitions to low-lying states. One argument against this explanation is that the higher n values are observed for (p, n) reactions in many regions of the Periodic Table²⁶; if this explanation were valid, it would be expected that anomalous values of n

would not be observed in regions where the shells nearest the Fermi level were characterized by low angular momentum values. An additional objection to invoking angular momentum as a cause for anomalous spectral shapes is that even the combination of a $g_{9/2}$ particle with a $g_{7/2}$ hole can produce angular momentum values no larger than $J=8$; examination of the transmission coefficients for protons and neutrons of the appropriate energies indicates that the values are above 0.5 for $l=4$ or 5 for protons or neutrons, respectively, implying that the inhibition of the population of even a $J=8$ state ought not be severe.

The discussion to this point has considered the effects of shells, pairing, and contributions from higher exciton states separately. A more detailed analysis would have to include the interaction between these phenomena. Because the effects of shell closure and pairing shifts are to reduce the density of proton-particle-neutron-hole states at low excitation energy, the result is that reactions involving higher exciton states are more likely to produce contributions to the hard portion of the spectrum. The pairing force, for example, will depress two (paired) particle-two (paired) hole states relative to one-particle-one-hole states with the result that contributions from higher exciton states may not decrease as rapidly as implied by Eq. (1).

Definitive identification of the causes of anomalous shapes for pre-equilibrium spectra awaits more extensive studies including nuclei more distant from closed shells. The present data suggest that shell effects, pairing effects, and contributions from higher exciton states all play a role in modifying the shape of the energy distribution;

angular momentum effects apparently have much less influence on the spectral shapes.

IV. SUMMARY

Examination of the pre-equilibrium neutron spectra produced in the $^{112}\text{Cd}(p, n)$, $^{113}\text{Cd}(p, n)$, $^{114}\text{Cd}(p, n)$, and $^{115}\text{In}(p, n)$ reactions has indicated that significant differences in spectral shape occur for neighboring nuclei. Since these nuclei are close to the $Z=50$ closed shell, one logical explanation for these variations would be shell effects. Calculations with a Nilsson single-particle basis predicted large shell effects only for the $^{115}\text{In}(p, n)^{115}\text{Sn}$ reaction; this result agrees qualitatively with the data. More subtle discrepancies between the spectra of the Cd isotopes and the exciton-model prediction are tentatively attributed to pairing effects. Again, qualitative agreement between the magnitudes of the predicted discrepancies and those observed in the data is obtained. The possible role of angular momentum in changing the energy distribution of emitted pre-equilibrium neutrons is also considered. It is concluded that no convincing evidence for significant angular momentum effects can be found in the present data. Although differences are observed between spectral shapes for adjacent isotopes, these are not in agreement with the predictions of the simple exciton model and agree only qualitatively with the analysis of Lee and Griffin. Similar studies (including particularly nuclei further from closed shells) would clearly aid in determining the relative influence of the above factors in modifying the shape of pre-equilibrium spectra.

*Work performed under the auspices of the U. S. Atomic Energy Commission.

¹J. J. Griffin, Phys. Rev. Letters 17, 478 (1966).

²M. Blann, Phys. Rev. Letters 21, 1357 (1968).

³V. V. Verbinski and W. R. Burrus, Phys. Rev. 177, 1671 (1969).

⁴M. Blann and F. M. Lanzafame, Nucl. Phys. A142, 559 (1970).

⁵F. C. Williams, Jr., Phys. Letters 31B, 184 (1970).

⁶S. M. Grimes, J. D. Anderson, J. W. McClure, B. A. Pohl, and C. Wong, Phys. Rev. C 3, 645 (1971).

⁷C. K. Cline and M. Blann, Nucl. Phys. A172, 225 (1971).

⁸R. Bimbot and Y. Le Beyec, J. Phys. (Paris) 32, 243 (1971).

⁹M. Chevarier, A. Chevarier, A. Demeyer, and Tran Min Duc, J. Phys. (Paris) 32, 483 (1971).

¹⁰A. Veyssiere, H. Beil, R. Bergere, P. Carlos, and A. Lepretre, Nucl. Phys. A159, 561 (1970).

¹¹C. Birattari, E. Gadioli, A. M. Grassi Strini, G. Strini, G. Tagliaferri, and L. Zetta, Nucl. Phys. A166, 605 (1971).

¹²G. D. Harp and J. M. Miller, Phys. Rev. C 3, 1847 (1971).

¹³E. Gadioli, I. Iori, N. Molho, and L. Zetta, Phys. Rev. C 4, 1412 (1971).

¹⁴L. Milazzo-Colli and M. G. Braga-Marcazzan, Phys. Letters 36B, 447 (1971).

¹⁵C. K. Cline, Nucl. Phys. A174, 73 (1971).

¹⁶S. M. Grimes, J. D. Anderson, B. A. Pohl, J. W. McClure, and C. Wong, Phys. Rev. C 4, 607 (1971).

¹⁷M. Blann, Phys. Rev. Letters 27, 337 (1971).

¹⁸E. V. Lee and J. J. Griffin, Phys. Rev. C 5, 1713 (1972).

¹⁹R. M. Wood, R. R. Borchers, and H. H. Barschall, Nucl. Phys. 71, 529 (1965).

²⁰J. D. Anderson and C. Wong, Nucl. Instr. Methods 15, 178 (1962); B. D. Walker, J. D. Anderson, J. W. Mc-

Clure, and C. Wong, *ibid.* **29**, 333 (1964).

²¹S. G. Nilsson, Kgl. Danske Videnskab. Selskab, Mat.-Fys. Medd. **29**, No. 16 (1955).

²²A computer code (written by F. C. Williams, Jr.) in use at the University of Rochester for such calculations was kindly supplied to the authors by Professor M. Blann.

²³C. M. Lederer, J. M. Hollander, and I. Perlman, *Table of Isotopes* (Wiley, New York, 1967), p. 591.

²⁴P. H. Stelson and L. Grodzins, Nucl. Data **A1**, 21 (1965).

²⁵A. Gilbert and A. G. W. Cameron, Can. J. Phys. **43**, 1446 (1965).

²⁶S. M. Grimes, Bull. Am. Phys. Soc. **16**, 550 (1971); Lawrence Livermore Laboratory Report No. UCRL 73152, 1971 (unpublished).

PHYSICAL REVIEW C

VOLUME 7, NUMBER 1

JANUARY 1973

Magnetic Moment of the 80-keV 1^- State of ^{144}Pr

B. K. Sinha and R. Bhattacharyya

Saha Institute of Nuclear Physics, Calcutta, India

(Received 8 March 1972)

The magnetic moment of the 80-keV 1^- state of ^{144}Pr has been determined using the integral-reversed-field method of the perturbed angular correlations. The value of $\mu = (-4.3 \pm 1.4)\mu_N$ indicates a structure of the 80-keV level based on the mixing between two shell-model states, both having the odd neutron in $f_{7/2}$ configuration—the odd proton occupying $g_{7/2}$ and $d_{5/2}$ configurations, respectively.

I. INTRODUCTION

The decay of $^{144}\text{Ce} \rightarrow ^{144}\text{Pr}$ has been the subject of a number of studies in recent years.¹⁻³ This is because of the fact that the long half-life of ^{144}Ce makes the odd-odd nucleus ^{144}Pr one of those few which lends itself to prolonged study. The position of the nucleus ^{144}Pr in the mass region just outside the well-known deformed region $150 \leq A \leq 190$ is also important. The first precise determination of the energy levels and their spin-parities and the multipolarities of the γ transitions amongst them was made by Geiger, Graham, and Ewan⁴ with the help of an iron-free $\pi\sqrt{2}$ β spectrometer. These authors conclude that, whereas the single-particle shell model fails to account for the spin-parities of the levels of ^{144}Pr , a unified-model interpretation in terms of the intrinsic odd-nuclear level assignments of Mottelson and Nilsson (assuming a prolate deformation $\delta \approx +0.07$ and with qualitative restrictions on the possible odd-neutron and odd-proton level combinations) is successful in providing an unique selection of the spin-parities of the energy levels. However, the authors predicted on this basis a lifetime for the 59-keV first excited state of ^{144}Pr of the order of 3 sec which we now know to be about 7 min.¹ In particular, Geiger, Graham, and Ewan⁴ proposed that the spin-parity of the 80-keV levels arises from the coupling of the component of the proton angular momentum $\Omega_p = \frac{5}{2}^+$ and neutron angular momentum $\Omega_n = \frac{3}{2}^-$ along the nuclear symmetry axis. Burde, Rakavy, and Engler⁵ measured the lifetime of the different levels by β - γ coincidence techniques and

found that the different γ -transition probabilities agree very well with those of the shell-model calculations in terms of coupling between odd neutron and odd proton using effective moments from neighboring odd-neutron and odd-proton nuclei. These authors conclude that the 80-keV 1^- state of ^{144}Pr is composed of a mixture of two shell-model states both having the odd neutron in the $f_{7/2}$ configuration (the odd proton occupying $g_{7/2}$ and $d_{5/2}$ configurations, respectively).

The γ - γ ⁶⁻¹⁰ and β - γ ^{11, 12} angular correlations have also been performed on the various cascades of ^{144}Pr to find out the nature of the levels excited in the decay of ^{144}Ce (Fig. 1). However, we have not come across any mention of the measurement of the magnetic moment of any level of ^{144}Pr in the existing literature. The present investigation is therefore expected to throw more light upon the situation.

II. EXPERIMENTAL ARRANGEMENT

The detectors were RCA-6810A photomultipliers with 3.8-cm-diam \times 3.8-cm-thick NaI(Tl) crystals coupled to them. Magnetic shielding was provided by using mu-metal shields together with layers of netic and conetic wrappings. The coincidence resolving time was 20 nsec. The magnetic field used was 23.3 kG which was measured by a Beckman Hall probe calibrated in a nuclear magnetic resonance setup. The source used was cerous chloride in dilute HCl obtained from Bhabha Atomic Research Center, Trombay, India. Since the Pr^{3+} ion is paramagnetic, the temperature of the source was maintained reasonably steady at